Published in final edited form as:
J Am Chem Soc. 2008 September 24; 130(38): 12656–12662. doi:10.1021/ja7111146.

Inhibition of Class A β-Lactamases by Carbapenems: Crystallographic Observation of Two Conformations of Meropenem in SHV-1

Michiyosi Nukaga[†], **Christopher R. Bethel**[‡], **Jodi M. Thomson**[§], **Andrea M. Hujer**[‡], **Anne Distler**[§], **Vernon E. Anderson**[‖], **James R. Knox**[⊥], and **Robert A. Bonomo**[*,‡,§]
Faculty of Pharmaceutical Sciences, Josai International University, Togane City, Chiba 283-8555, Japan; Research Service, Veterans Affairs Medical Center, Cleveland, Ohio 44106; Departments of Pharmacology and Biochemistry, Case School of Medicine, Cleveland, Ohio 44106; Department of Molecular and Cell Biology, University of Connecticut, Storrs, Connecticut 06269

Abstract

Carbapenem antibiotics are often the “last resort” in the treatment of infections caused by bacteria resistant to penicillins and cephalosporins. To understand why meropenem is resistant to hydrolysis by the SHV-1 class A β-lactamase, the atomic structure of meropenem inactivated SHV-1 was solved to 1.05 Å resolution. Two conformations of the Ser70 acylated intermediate are observed in the SHV-1-meropenem complex; the meropenem carbonyl oxygen atom of the acyl-enzyme is in the oxyanion hole in one conformation, while in the other conformation it is not. Although the structures of the SHV-1 apoenzyme and the SHV-1-meropenem complex are very similar (0.29 Å rmsd for Cα atoms), the orientation of the conserved Ser130 is different. Notably, the Ser130-OH group of the SHV-1-meropenem complex is directed toward Lys234Nz, while the Ser130-OH of the apo enzyme is oriented toward the Lys73 amino group. This altered position may affect proton transfer via Ser130 and the rate of hydrolysis. A most intriguing finding is the crystallographic detection of protonation of the Glu166 known to be involved in the deacylation mechanism. The critical deacylation water molecule has an additional hydrogen-bonding interaction with the OH group of meropenem’s 6α-1*R*-hydroxyethyl substituent. This interaction may weaken the nucleophilicity and/or change the direction of the lone pair of electrons of the water molecule and result in poor turnover of meropenem by the SHV-1 β-lactamase. Using timed mass spectrometry, we further show that meropenem is covalently attached to SHV-1 β-lactamase for at least 60 min. These observations explain key properties of meropenem’s ability to resist hydrolysis by SHV-1 and lead to important insights regarding future carbapenem and β-lactamase inhibitor design.

[*]robert.bonomo@med.va.gov.
[†]Josai International University.
[‡]Veterans Affairs Medical Center.
[§]Department of Pharmacology, Case School of Medicine.
[‖]Department of Biochemistry, Case School of Medicine.
[⊥]University of Connecticut.

Introduction

Carbapenem antibiotics (imipenem **1**, meropenem **2**, ertapenem **3** and doripenem **4**, Figure 1) possess the broadest antibacterial spectrum of all β-lactams.[1,2] As intravenous formulations, carbapenems are primarily used in the treatment of serious nosocomially acquired infections caused by penicillin and cephalosporin resistant bacteria.[2] Their notable clinical success is due to two unique properties: (i) carbapenems resist hydrolysis by most serine β-lactamases; and (ii) carbapenems possess remarkable affinity for Gram-positive and Gram-negative penicillin binding proteins (PBPs), the target transpeptidases and carboxypeptidases used by bacteria to construct cell walls.[3,4] Among the more than 700 β-lactamases found in nature (Dr. K. Bush, personal communication) only a few are able to inactivate carbapenems.[5-18] The impact of these bacterial inactivating enzymes (e.g., KPC-2, NMC-A, SME, OXA-23, CMY-10, GES-2, IMP-2, and VIM-2) on the "clinical longevity" of our current and future carbapenems demands close attention as many health care centers are reporting carbapenem resistant Gram-negative clinical isolates.[19]

The stability of imipenem **1** to hydrolysis by class A β-lactamases was first noted in the study of the class A β-lactamase of *Bacillus cereus*.[20] Imipenem behaved as a "slow substrate" that reacted by a branched pathway mechanism.[20] Using a β-lactamase that is of contemporary clinical importance, Tiabi and Mobashery found that the rate constant for hydrolysis of imipenem by TEM-1 was reduced by 50000-fold compared to benzylpenicillin. The tautomerization of the double bond ($\Delta^2 \rightarrow \Delta^1$) in the acyl enzyme attenuated the rate of deacylation thereby resulting in a biphasic turnover profile with Arg244 playing an important role.[21,22] The extreme reduction in the deacylation rate was determined to be largely due to the interactions of the 6α-1*R*-hydroxyethyl group of imipenem with TEM-1.[21] The crystal structure of imipenem bound to TEM-1 (Protein Data Bank code 1BT5) revealed an acylserine enzyme is formed (Scheme 1) and that the hydroxyethyl group forces imipenem to adopt a conformation in which the carbonyl oxygen of the acylserine bond is flipped out from its expected location in the oxyanion pocket.[19]

This dramatic conformational change appears to be a result of steric constraints between the large substituent at the C_6 position and the Ser130-Asp131-Asn123 (SDN) loop. These destabilizing interactions provided a structural rationale for the biphasic kinetics and significant reduction in deacylation rate.

To further investigate the importance of steric interactions between the 6α-1*R*-hydroxyethyl group of imipenem and TEM-1 β-lactamase, the Asn132Ala variant of TEM-1 β-lactamase was engineered.[23] In this complex (PDB 1JVJ), the imipenem intermediate adopts a very different conformation from that observed in the TEM-1-imipenem structure. The destabilizing interactions with residue Asn132 are relieved, supporting the importance of the earlier observations made by Maveyraud et al.[19]

Similarly, the class C AmpC β-lactamase of *Escherichia coli* inactivated by imipenem forms a covalent complex in the active site.[24] This structure (PDB 1LL5) demonstrates that imipenem is bound to Ser64 and that the carbonyl oxygen of the acylserine bond was not positioned in the oxyanion hole; imipenem was rotated 180°, moved approximately 3 Å

away from its expected location and adopts a conformation similar to that seen in the TEM-1-imipenem complex.[24]

The crystal structure of meropenem inactivating OXA-13 β-lactamase, a class D extended-spectrum serine β-lactamase, shows that meropenem is covalently attached to the reactive Ser67 and there is a salt bridge involving the C_3 carboxylate of meropenem and Arg250 (PDB 1H8Y).[25,26] In the apo and complexed form, an "unsuspected conformational flexibility" in the area of the conserved Ser115 residue was detected. It was observed that the 114–116 loop (equivalent to the 130–132 SDN loop of TEM-1 and SHV-1) moved 3.5 Å toward the side-chain of Lys70 (equivalent to Lys73).[26]

Intrigued by these prior studies and the description in 2003 of a carbapenem hydrolyzing class A SHV β-lactamase (SHV-38),[13] we focused our attention on the interactions of meropenem **2** with SHV family β-lactamases.[27] Meropenem served an important role as a substrate/inhibitor in our analysis of the function of the $C_{3–4}$ carboxylate in β-lactam affinity for SHV-1.[27] Interestingly, at that time we could not demonstrate any turnover of meropenem by SHV-1.[27] Therefore, we hypothesized that meropenem acted as a direct, irreversible inactivator of SHV-1 β-lactamase. These observations compelled us to determine the crystal structure of the reaction intermediate for meropenem with the SHV-1 β-lactamase to explain both its affinity and its resistance to hydrolysis.

Materials and Methods

Purification and Crystallization

The methods for purification and crystallization of SHV-1 were previously described.[28-30] In brief, SHV-1 was purified to homogeneity from *Escherichia coli* DH10B cells according to a method employing preparative isoelectric focusing.[31-33]

The sitting-drop vapor diffusion method was applied for ligand-free SHV-1 crystallization at room temperature.[29,30] A 10 μL crystallization drop [containing 2.5 mg/mL protein, 0.56 mM 6-cyclohexyl-1-hexyl-β-D-maltoside (Cymal-6) detergent (Anatrace, Masume, OH), 15% polyethylene glycol (PEG) 6000, and 50 mM HEPES (Sigma Chemical Co., St. Louis, MO.) buffer (pH 7.0)] was placed over a 0.75 mL reservoir solution [30% PEG 6000 and 0.1 M HEPES (pH 7.0)].

Meropenem was obtained from AstraZeneca Pharmaceuticals (Mt. Prospect, IL) as a kind gift. A pregrown crystal of SHV-1 was soaked at 21 °C for 90 min in a PEG holding solution (30% PEG 6000, 0.56 mM Cymal-6 and 50 mM HEPES pH 7.0) containing 2 mM meropenem. A half-volume of the soaking solution was refreshed every 30 min.

Kinetics

The dissociation constant for the preacylation complex, K_d, of meropenem for SHV-1 β-lactamase and the turnover number (activity remaining after 24 h of inactivation) were previously reported.[27]

Electrospray Ionization Mass Spectrometry (ESI-MS)

Using ESI-MS, SHV-1 and SHV-1 β-lactamase inactivated with meropenem were studied. In the case of SHV-1, meropenem, the resulting mixture was analyzed at 0, 15, 30, and 60 min. In these experiments we employed 40 μM of SHV-1 β-lactamase and 20 mM of meropenem in phosphate buffered saline, pH 7.4. The mixture (inhibitor, *I*, to enzyme, *E*, of 500:1) was equilibrated with 0.1% trifluoroacetic acid (TFA) and desalted using a C_{18} ZipTip (Millipore, Bedford, MA). SHV-1 was also equilibrated with 0.1% trifluoroacetic acid (TFA) and desalted using C_{18} ZipTip according to the manufacturer's protocol. Samples were then placed on ice and analyzed within 10 min.

Spectra of the intact SHV-1 and SHV-1: meropenem were generated on an Applied Biosystems (Framingham, MA) Q-STAR XL quadrupole-time-of-flight (TOF) mass spectrometer equipped with a nanospray source. Experiments were performed by diluting the protein sample with acetonitrile/1% formic acid to a concentration of 10 μM. This protein solution was then infused at a rate of 0.5 μL/min and data were collected for 2 min. Spectra were deconvoluted using the Applied Biosystems (Framingham, MA) Analyst program.

X-ray Data Collection

The meropenem-soaked SHV-1 crystal was cryoprotected by the addition of 25% 2-methyl-2,4-pentanediol (MPD) to the PEG holding solution. Loop-mounted crystals were flash-cooled and kept at 100 K with a nitrogen gas stream (Oxford Cryosystems, Oxford, U.K.). The 0.5-degree oscillation images were collected on a Q210 CCD detector (Area Detector Systems Corp., Poway, CA) at the Cornell High Energy Synchrotron Source (MacCHESS). Only one crystal was used. The HKL programs were used to reduce and scale X-ray intensities (Table 1).[34]

Results and Discussion

Structure Determination and Refinement

The 28.9 kDa SHV-1 β-lactamase crystallized in space group $P2_12_12_1$ with one molecule in the asymmetric unit and the following cell dimensions: $a = 49.6$, $b = 55.6$, and $c = 87.0$ Å (100 K). Using the apo SHV-1 structure (PDB 1SHV) as a model,[29] initial rigid-body refinement was accomplished with CNS.[35] A simulated annealing protocol with 2 Å data and cross validation using R_{free} were then used in the refinements.[36] XtalView was employed for structure and map displays and for manual manipulation of the structures.[37] At this stage *R* factors were ca. 25% for the unhydrated SHV-1 apo protein model. As the protein model was being optimized and hydrated, a large serine bound structure with the acylserine-group in two different conformations became clear in the difference density map.

The final stages of the refinement were performed with SHELX[38] using all $F > 0\sigma(F)$ in steps to the highest resolution (Table 2). With highest resolution data, anisotropic B-factors were introduced. *R* factor and R_{free} values were reduced from 23.0/25.6 (%) to 15.5/18.2 (%). The validity of this step in the refinement was verified with PARVATI, a program that analyses the modeled anisotropy.[39] The mean anisotropy and σ for protein atoms were 0.434

and 0.099, respectively. Riding hydrogen atoms were later added in calculated positions. The refined occupancies of the two conformers of the serine-bound meropenem intermediate are 0.50 and 0.50. Atoms in the R′ side chain of meropenem beyond the sulfur atom were disordered and could not be modeled.

Comparison with Apo-β-lactamase Structure and the Role of the R′ side chain of Meropenem

The overall structure of the SHV-1 apo enzyme[29] and its meropenem complex (Figure 2) are very similar (rms deviation is 0.29 Å for Cα atoms). Earlier work showed that in the TEM-1 and AmpC-imipenem complexes, the inhibitor's carbonyl group was not bound in the oxyanion hole.[19,24] In contrast, for TEM-1 Asn132Ala, the imipenem is entirely bound in the oxyanion hole.[23] Our observations of the SHV-1-meropenem complex reveal that two conformations of the serine-bound intermediate exist (Figure 3). One of the conformers has its carbonyl group bound in the oxyanion hole, while the other conformer does not. In the first case, the carbonyl oxygen is hydrogen bonded to the NH amides of Ala237 and Ser70. In the second case, the carbonyl oxygen orients in another direction. Why in the SHV-1-meropenem complex are two conformations of the acylserine intermediate seen? Although the R′ side chains are positioned very differently in both the TEM-1 and TEM-1 Asn132Ala mutant-imipenem complexes, they are completely ordered (Figure 4). In the SHV-1-meropenem complex, we observe that the (carbamoyl)pyrrolidinyl group in R′ is disordered, possibly because the SHV-1 binding site is slightly larger than that in TEM-1.[29] This allows us to suggest that stabilizing interactions of the R′ side chain are required for optimum alignment of the acylserine group with the two amides forming the oxyanion hole.

Binding-Site Structure: Alteration of Arg244, Ser130, and Tyr105

When the SHV-1-meropenem complex is superimposed on the crystal structure of the apo SHV-1 β-lactamase, several changes are seen in active site residues. First, the orientation of the guanidinium group of Arg244 is slightly changed in order to interact with the C_3 carboxylate of meropenem. In this position, we note that one oxygen atom of the carboxylate group is hydrogen bonded to both Arg244:Nη^2 (2.71 Å) and Thr235: Oγ^2 (3.01 Å); the other oxygen atom is hydrogen bonded to Arg244:Nη^1 via W502 (2.67 Å) (Figure 3, 4a). A similar hydrogen bonding network around the carboxylate is observed in the TEM-1–imipenem (Figure 4b) and TEM-1–Asn132Ala–imipenem complexes (Figure 4c).[23] As Arg244 is highly conserved in class A β-lactamases, this configuration might contribute to the stability of carbapenem in the inactivation of class A enzymes and play a role in affinity.

More importantly, the Ser130 side chain is reoriented by 110°. In the apo SHV-1 enzyme, the main conformation of Ser130: Oγ is oriented toward Lys73 in the active site. The Ser130 hydroxyl group of the meropenem complex is pointed away from the active site pocket toward Lys234 on the B3 strand. In a manner reminiscent of what was seen in the TEM-1–imipenem structure (Figure 4b),[19] we observe that Lys234:Nε and the Ser130 hydroxyl group form strong hydrogen bonds (2.83 and 2.77 Å for two conformations of Lys234:Nε) and a hydrogen bond to W503 (2.59 Å). This resembles a second conformation that was observed in the SHV-2 apo structure and the TEM-1–imipenem structure.[19,30] Ser130 is absolutely conserved in all class A B-lactamases and known to assist catalysis, chiefly by

proton transfer to N_4 in the acylation step. Although reorientation of Ser130 is a major change in the active site pocket, the apparent impact on the meropenem acyl-enzyme is limited.

Surprisingly, we detected that the side chain of Tyr105 is repositioned. Two conformations of Tyr105 are observed; one is similar to the conformation of the apo enzyme and the other is similar to the TEM-1–imipenem complex.[19] Compared with other active-site residues, the map quality of the Tyr105 ring is poor. This suggests the mobility of Tyr105 in these two conformations may be linked to the bimodal positioning of meropenem in the oxyanion hole. In fact, the occupancies of the two Tyr105 conformers (0.40 and 0.60 see below) are about the same as those of the meropenem conformers (0.50 and 0.50), so that a correlation in positions is possible. This observation supports a hypothesis raised previously that the loop containing Asp104Glu and -Lys and Tyr105 in SHV plays a key role in substrate and inhibitor interactions.[31]

Deacylation Water Molecule; Timed Mass Spectrometry

Why is the deacylation of the meropenem intermediate by SHV-1 so prolonged? Using steady state kinetics, we were unable to demonstrate if the change from conformer 1 (carbonyl oxygen in the oxyanion hole) to 2 (carbonyl oxygen out of the oxyanion hole) of meropenem in SHV-1 is associated with biphasic kinetics in the turnover of meropenem by SHV-1.[27] To assess the longevity of the acyl enzyme complex, we performed timed mass spectrometry experiments. This analysis reveals persistence of the acyl-enzyme for at least 60 min (Figure 5). Furthermore, we were not able to show recovery of SHV-1 activity after 24 h. To understand this, we examined the environment and interactions of the deacylation water in this complex.

The interactions of the deacylation water (W501) in the catalytic site are shown in Figure 6 and Table 3. We note that the deacylation water molecule and neighboring Glu166 and Asn170 side chains in the SHV-1 meropenem complex are located in the same position as in the apo structure. The hydroxyl group of the hydroxyethyl substituent is located very close to W501 (2.54 Å), suggesting a strong hydrogen bond. This hydrogen bond, as well as two others to Glu166 and Asn170, have been thought to decrease the nucleophilicity of deacylation water and thus explain the stability of carbapenems in TEM type β-lactamases.[40]

The most intriguing finding in this high resolution SHV-1: meropenem structure is the detection of the hydrogen atom belonging to the carboxylic acid group of Glu166 (Figure 6). The *Fo–Fc* peak between the deacylation water and Glu166: Oϵ^2 could be observed at a contour level of 3σ. The peak is closer to Glu166:Oε^2 (1.32 Å) than W501:O (1.69 Å), strongly suggesting a protonated Glu166 in the complex. Other protons which may hydrogen bond were not observed. Thus the protonated Glu166 establishes limits on the hydrogen bonding network, most likely as shown in Figure 7a. This finding is reminiscent of the discovery of a protonated Glu166 in the ultrahigh resolution (0.9 Å) structure of TEM-1:boronic acid derivative which is the analogue of the tetrahedral intermediate in acylation (PDB 1 M40).[40] In that study, and in work on the ultrahigh resolution structure of the apo SHV-2 (PDB 1N9B),[30] it is suggested that Glu166 acts as general base which deprotonates the Ser70 OH group via a deacylation water (catalytic water). After forming a

tetrahedral intermediate, the β-lactam ring is opened and a proton is transferred to N_4 of the β-lactam (Scheme 1). In the case of substrates that are readily hydrolyzed (such as ampicillin or amoxicillin), a hydrogen bond network could be formed in which the deacylation water hydrogen bonds only to the deprotonated Glu166 and Asn170 (Figure 7b). In the case of carbapenem type inhibitors, W501 forms three strong hydrogen bonds in this network. The addition of the third hydrogen bond would reduce the nucleophilicity of the deacylation water and further contribute to the longevity of SHV-1: meropenem acyl enzyme complex. A protonated Glu166 would be stabilized by introducing the OH group of the meropenem hydroxyethyl substituent very close to deacylation water. This event is the driving force for reformation of the hydrogen bond network around the deacylation water.

Concluding Remarks

We report the atomic structure of a class A SHV-1 β-lactamase inhibited by meropenem. This high resolution crystallographic analysis shows two conformations of the inhibitor in the active site, reveals key movements of the Ser130 hydroxyl, Tyr105, and Arg244 residues, and demonstrates rearrangements of the hydrogen bond network around the critical deacylation water. Our analysis is further supported by timed mass spectrometry that reveals the prolonged presence of the acyl-enzyme species. These studies provide unique insights into meropenem's distinctive behavior as a β-lactamase inhibitor of SHV family enzymes. More importantly, we show key differences between meropenem inhibition of class A SHV-1 and the imipenem inhibition of (i) class A TEM-1 and its variants, (ii) class C AmpC β-lactamase, and (iii) meropenem/imipenem inhibition of class D OXA-13. These variations largely involve exclusive structural interactions in SHV-1 that only become evident with the formation of the meropenem-SHV-1 acyl-enzyme complex. Yet, an overriding theme emerges. In each of the structures cited, meropenem (or imipenem) induces β-lactamase conformational changes and hydrogen bond rearrangements that result in catalytically impaired serine enzymes. This ligand induced remodeling and repositioning of active site residues represents an alternative strategy to inhibit β-lactamases. Our studies lead us to anticipate that substrates/inhibitors can be designed that can capitalize on remodeling the active site serine β-lactamases in critical ways and interfere with substrate turnover.

Acknowledgments

The Veterans Affairs Merit Review Program and the National Institutes of Health (Grant RO1 AI063517-01) supported these studies. J.M.T. is supported by NIH Grant T32 GM07250 and the Case Medical Scientist Training Program. These studies were partly supported by the Grant-in-Aid for Scientific Research (C), No. 17590090, Japan Society for the Promotion of Science and the Futaba Electronics Memorial Foundation. We thank the staff of the Macromolecular Diffraction Facility (MacChess) at Cornell University for assistance with x-ray data collection. Atomic coordinates have been deposited in the Protein Data Bank as entry 2ZD8.

References

(1). Lee VJ, Miller GH, Yagisawa M. Curr. Opin. Microbiol. 1999; 2:475–482. [PubMed: 10508732]

(2). Quinn JP. Diagn. Microbiol. Infect. Dis. 1998; 31:389–395. [PubMed: 9635914]

(3). Fisher JF, Meroueh SO, Mobashery S. Chem. Rev. 2005; 105:395–424. [PubMed: 15700950]

(4). Bush K, Mobashery S. Adv. Exp. Med. Biol. 1998; 456:71–98. [PubMed: 10549364]

(5). Bratu S, Tolaney P, Karumudi U, Quale J, Mooty M, Nichani S, Landman D. J. Antimicrob. Chemother. 2005; 56:128–132. [PubMed: 15917285]

(6). Helfand MS, Bonomo RA. Curr. Drug Targets Infect. Disord. 2003; 3:9. [PubMed: 12570729]
(7). Kim JY, Jung HI, An YJ, Lee JH, Kim SJ, Jeong SH, Lee KJ, Suh PG, Lee HS, Lee SH, Cha SS. Mol. Microbiol. 2006; 60:907–916. [PubMed: 16677302]
(8). Livermore DM. J. Antimicrob. Chemother. 1992; 29(6):609–613. [PubMed: 1506344]
(9). Livermore DM. Curr. Opin. Investig. Drugs. 2002; 3:218–224.
(10). Livermore DM, Woodford N. Trends Microbiol. 2006; 14:413–420. [PubMed: 16876996]
(11). Nordmann P, Poirel L. Clin. Microbiol. Infect. 2002; 8:321–331. [PubMed: 12084099]
(12). Paterson DL. Semin. Respir. Infect. 2002; 17:260–264. [PubMed: 12497542]
(13). Poirel L, Heritier C, Podglajen I, Sougakoff W, Gutmann L, Nordmann P. Antimicrob. Agents Chemother. 2003; 47:755–758. [PubMed: 12543688]
(14). Poirel L, Pitout JD, Nordmann P. Future Microbiol. 2007; 2:501–512. [PubMed: 17927473]
(15). Poirel L, Weldhagen GF, Naas T, De Champs C, Dove MG, Nordmann P. Antimicrob. Agents Chemother. 2001; 45:2598–2603. [PubMed: 11502535]
(16). Poirel L, Wenger A, Bille J, Bernabeu S, Naas T, Nordmann P. Antimicrob. Agents Chemother. 2007:2282–2283. [PubMed: 17420208]
(17). Walsh TR, Toleman MA, Poirel L, Nordmann P. Clin. Microbiol. Rev. 2005; 18:306–325. [PubMed: 15831827]
(18). Walther-Rasmussen J, Hoiby N. J. Antimicrob. Chemother. 2006; 57:373–383. [PubMed: 16446375]
(19). Maveyraud L, Mourey L, Kotra LP, Pedelacq J-D, Guillet V, Mobashery S, Samama J-P. J. Am. Chem. Soc. 1998; 120:9748–9752.
(20). Monks J, Waley SG. Biochem. J. 1988; 253:323–328. [PubMed: 3263117]
(21). Taibi P, Mobashery S. J. Am. Chem. Soc. 1995; 117:7600–7605.
(22). Zafaralla G, Mobasherry S. J. Am. Chem. Soc. 1992; 114:1505–1506.
(23). Wang X, Minasov G, Shoichet BK. Proteins. 2002; 47:86–96. [PubMed: 11870868]
(24). Beadle BM, Shoichet BK. Antimicrob. Agents Chemother. 2002; 46:3978–3980. [PubMed: 12435704]
(25). Mugnier P, Podglajen I, Goldstein FW, Collatz E. Microbiology. 1998; 144:1021–1031. [PubMed: 9579076]
(26). Pernot L, Frenois F, Rybkine T, L'Hermite G, Petrella S, Delettre J, Jarlier V, Collatz E, Sougakoff W. J. Mol. Biol. 2001; 310:859–874. [PubMed: 11453693]
(27). Thomson JM, Distler AM, Prati F, Bonomo RA. J. Biol. Chem. 2006; 281:26734–26744. [PubMed: 16803899]
(28). Kuzin AP, Nukaga M, Nukaga Y, Hujer A, Bonomo RA, Knox JR. Biochemistry. 2001; 40:1861–1866. [PubMed: 11327849]
(29). Kuzin AP, Nukaga M, Nukaga Y, Hujer AM, Bonomo RA, Knox JR. Biochemistry. 1999; 38:5720–7572. [PubMed: 10231522]
(30). Nukaga M, Mayama K, Hujer AM, Bonomo RA, Knox JR. J. Mol. Biol. 2003; 328:289–301. [PubMed: 12684014]
(31). Bethel CR, Hujer AM, Hujer KM, Thomson JM, Ruszczycky MW, Anderson VE, Pusztai-Carey M, Taracila M, Helfand MS, Bonomo RA. Antimicrob. Agents Chemother. 2006; 50:4124–4131. [PubMed: 16982784]
(32). Helfand MS, Bethel CR, Hujer AM, Hujer KM, Anderson VE, Bonomo RA. J. Biol. Chem. 2003; 278:52724–52729. [PubMed: 14534312]
(33). Hujer AM, Hujer KM, Bonomo RA. Biochim. Biophys. Acta. 2001; 1547:37–50. [PubMed: 11343789]
(34). Otwinowski Z, Minor W. Methods Enzymol. 1997; 276:307–326.
(35). Brunger AT, Adams PD, Clove GM, Delano WL, Gros P, Grosse-Kunstleve RW. Acta Crystallog., Sect. D. 1998; 57:488–497.
(36). Brunger AT. Nature. 1992; 355:472–475. [PubMed: 18481394]
(37). McRee DE. J. Struct. Biol. 1999; 125:156–165. [PubMed: 10222271]
(38). Sheldrick GM, Schneider TR. Methods Enzymol. 1997; 277:319–343. [PubMed: 18488315]

(39). Merritt EA. Acta Crystallogr., Sect. D. 1999; 55:1109–1117. [PubMed: 10329772]
(40). Minasov G, Wang X, Shoichet BK. J. Am. Chem. Soc. 2002; 124:5333–5340. [PubMed: 11996574]
(41). Kraulis PJ. J. Appl. Crystallogr. 1991; 24:946–950.
(42). Merritt EA, Murphy ME. Acta Crystallogr., Sect. D. 1994; 50:869–873. [PubMed: 15299354]

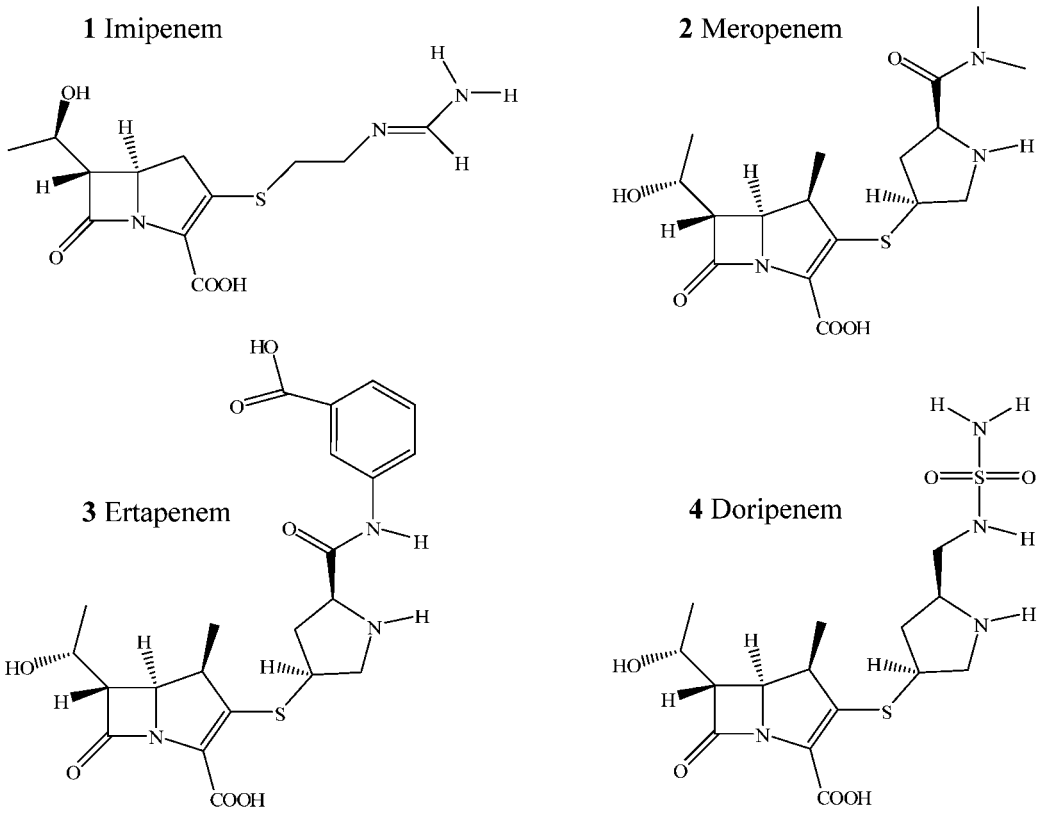

Figure 1.
Chemical structures of the four available carbapenems used in the clinic.

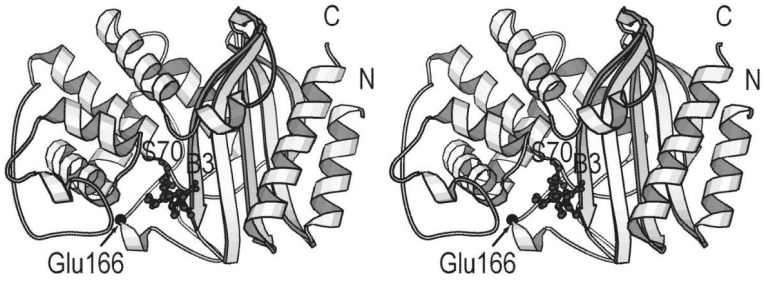

Figure 2.

Ribbon diagram of the SHV-1 β-lactamase complex with meropenem. Drawn by MOLSCRIPT.[41]

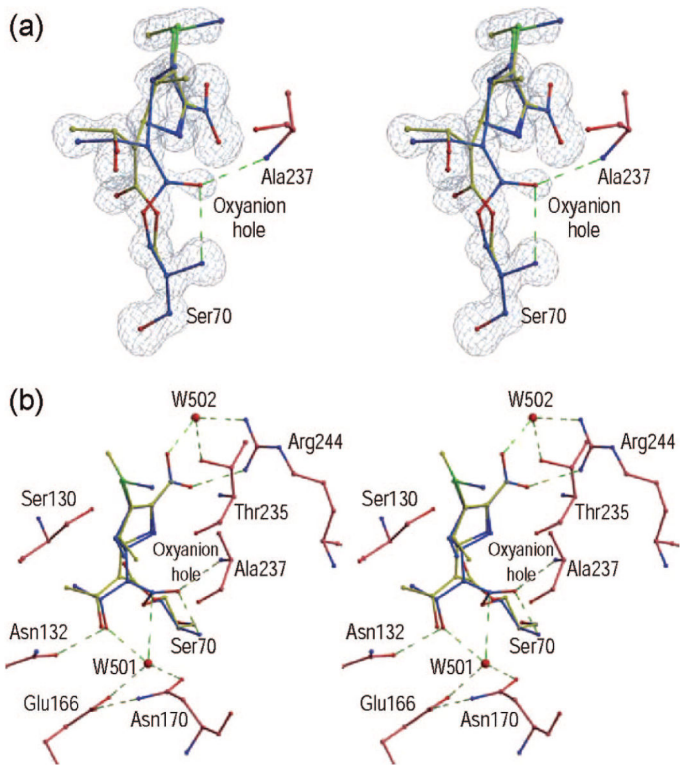

Figure 3.

(a) The *Fo–Fc* electron density at the 2.5σ contour level for the SHV-1:meropenem complex. Meropenem was omitted from the phase calculation. The carbonyl carbon atom of meropenem is covalently bonded to Ser70:Oγ but required modeling in two distinct conformations, one with the carbonyl oxygen atom bound in the oxyanion hole (its carbon atoms were colored blue) and the other with the carbonyl oxygen outside of the oxyanion hole (its carbon atoms were colored yellow). (b) The R′ side chain beyond the sulfur atom was disordered. Active site residues and water molecules in contact with meropenem are shown (pink). Figure was drawn with XtalView[37] and Raster3D.[42]

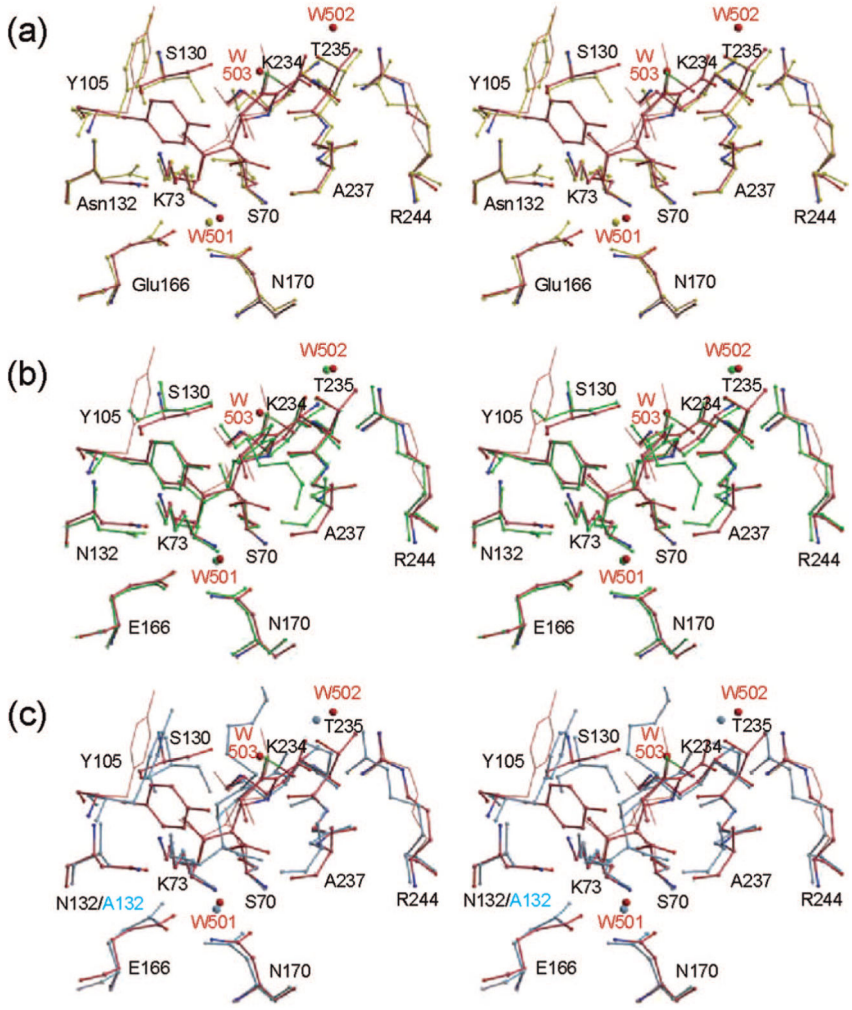

Figure 4.

(a) Stereoview of superposition of SHV-1: meropenem (PDB 2ZD8) and the SHV-1 apo (yellow, PDB 1SHV). (b) SHV-1:meropenem and TEM-1:imipenem (green, PDB 1BT5), (c) SHV-1:meropenem and TEM-1 Asn132Ala variant:imipenem (blue, PDB 1JVJ). In all three figures, the carbon atoms of SHV-1:meropenem complex were shown in pink. Their oxygen, nitrogen, and sulfur atoms were in red, blue, and green, respectively. The thin pink line indicates the second conformation of SHV-1:meropenem complex.

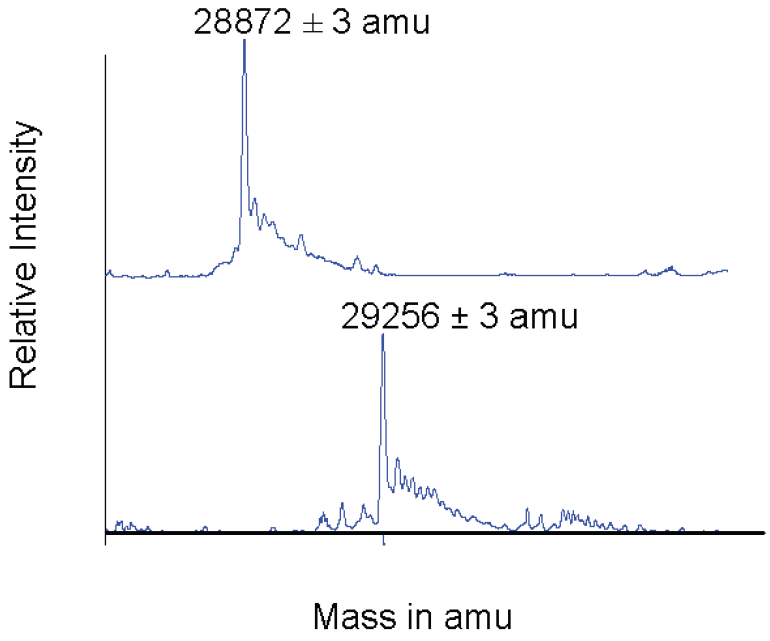

Figure 5.

The deconvoluted mass spectra of SHV-1 before (Figure 5a) and after 60-min inactivation with meropenem (Figure 5b). Spectra were obtained on a Q-STAR XL quadrupole-time-of-flight mass spectrometer equipped with a nanospray source. A single mass adduct is formed (Figure 5b).

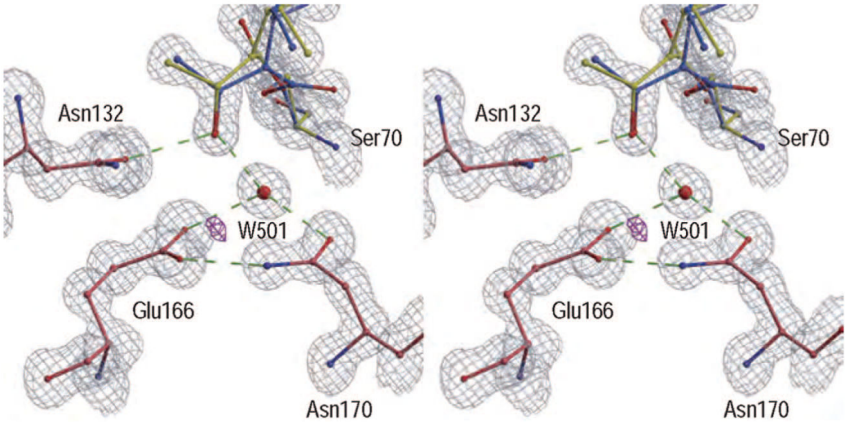

Figure 6.

Stereoview of electron density map around the deacylation water molecule W501. Original difference density for hydrogen atom (the atom was not modeled) between deacylation water and Glu166:Oε^2 (magenta, *Fo–F*c, contour level at 2.5σ) and neighborhood residue densities (gray, 2*Fo–Fc*, 1.5σ).Colors of active site residues and meropenem were the same as Figure 3.

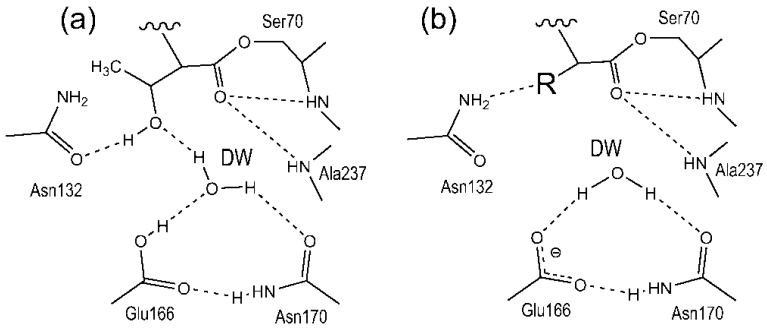

Figure 7.

Deduced hydrogen bond network around deacylation water for meropenem-bound acyl-enzyme (a) and a good substrate such as ampicillin (b).

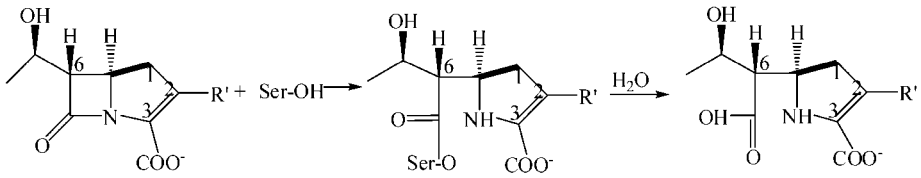

Scheme 1.

A Generalized Scheme Representing the Acyl-Enzyme Reaction between Class A β-Lactamase (e.g., TEM-1) and a Carbapenem

Table 1

X-ray Data Collection

space group	$P2_12_12_1$
cell constants	a = 49.29, b = 54.98, c = 85.63 (α = β = γ = 90°)
λ (Å)	0.9848
resolution (Å)	50–1.05 (1.05–1.07)[a]
observations	1525340 (28201)
unique reflections	105455 (5321)
R_{merge} [b]	0.086 (0.318)
completeness (%)	95.1 (67.8)
av $I/\sigma(I)$	18.7 (4.0)

[a] Data for highest resolution shell are in parentheses.

[b] $R_{merge} = \Sigma|I_{av} - I_i|/I_i$, where I_{av} is the average of all individual observations, I_i. The space group is $P2_12_12_1$.

Table 2

Results from SHELX Refinement

resolution range (Å)	30–1.05
no. of reflections used [$F > 0\sigma(F)$]	101, 163
R-factor/R_{free} [a] (%)	13.4/16.8
R_{total} (%)	13.5
residues in Ramachandran zone (%)	
favored/allowed	91.8/8.2
disallowed	0
rmsd values from ideality	
bond lengths (Å)	0.015
bond angles (Å)	0.032
zero chiral volumes (Å^3)	0.130
non-zero chiral volumes (Å^3)	0.153
mean B-factor (number of atoms)	
protein	12.8 (2103)
inhibitor	16.6 (31)
cymal-6	17.0 (45)
water molecules	29.6 (404)
all atoms	15.5 (2583)

[a] R_{free} was calculated from 3366 reflections.

Table 3

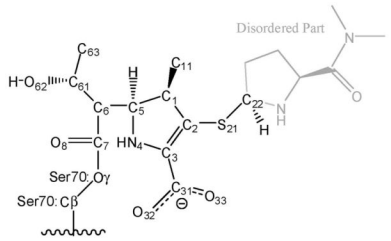

Interatomic Distances Around Deacylation Water (Å)	
Wat501:O–MER:O_{62} [a]	2.54
Wat501:O–MER:C_7 [b]	3.22
Wat501:O–E166Oε^2	2.59
Wat501:O–N170:Oδ^1	2.73
S70:N–MER:O_8 [c]	2.88
A237:N–MER:O_8	2.76
N132:Oδ^1–MER:O_{62}	2.68
Interatomic Angles around Deacylation Water (deg)	
MER:O_{62}–W501:O–E166:Oε^2	87.9
MER:O_{62}–W501:O–N170:Oδ^1	114.2
MER:O_{62}–W501:O–MER:C_7	52.9
E166:Oδ^2–W501:O–N170:Oδ^1	123.8
F166:Oε^2–W501:O–MER:C_7	131.0
N170:Oδ^1–W501:O–MER:C_7	100.9
N132:Oδ^1–MER:O_{62}–W501:O	106.2

[a] Oxygen atom of 6α-1-*R*-hydroxyethyl group of meropenem molecule.

[b] Carbonyl carbon atom in acyl group of oxyanion hole forming meropenem molecule (conformation A).

[c] Carbonyl oxygen atom in acyl group of oxyanion hole forming meropenem molecule (conformation A).